A *Drosophila* model of Fragile X syndrome exhibits defects in phagocytosis by innate immune cells

Reed M. O'Connor,[1]* Elizabeth F. Stone,[1]* Charlotte R. Wayne,[1] Emily V. Marcinkevicius,[1] Matt Ulgherait,[1] Rebecca Delventhal,[1] Meghan M. Pantalia,[1] Vanessa M. Hill,[1] Clarice G. Zhou,[4] Sophie McAllister,[4] Anna Chen,[4] Jennifer S. Ziegenfuss,[2] Wesley B. Grueber,[2] Julie C. Canman,[3] and Mimi M. Shirasu-Hiza[1]

[1]Department of Genetics and Development, [2]Department of Physiology and Cellular Biophysics, and [3]Department of Pathology and Cell Biology, Columbia University Medical Center, New York, NY 10032
[4]Department of Biological Sciences, Columbia University, New York, NY 10025

Fragile X syndrome, the most common known monogenic cause of autism, results from the loss of FMR1, a conserved, ubiquitously expressed RNA-binding protein. Recent evidence suggests that Fragile X syndrome and other types of autism are associated with immune system defects. We found that *Drosophila melanogaster Fmr1* mutants exhibit increased sensitivity to bacterial infection and decreased phagocytosis of bacteria by systemic immune cells. Using tissue-specific RNAi-mediated knockdown, we showed that Fmr1 plays a cell-autonomous role in the phagocytosis of bacteria. *Fmr1* mutants also exhibit delays in two processes that require phagocytosis by glial cells, the immune cells in the brain: neuronal clearance after injury in adults and the development of the mushroom body, a brain structure required for learning and memory. Delayed neuronal clearance is associated with reduced recruitment of activated glia to the site of injury. These results suggest a previously unrecognized role for Fmr1 in regulating the activation of phagocytic immune cells both in the body and the brain.

Introduction

The most common known monogenic cause of intellectual disability and autism in humans is Fragile X syndrome (Kelleher and Bear, 2008). In Fragile X syndrome, expansion of repeating DNA sequences in the genome induces transcriptional silencing of the highly conserved *FMR1* gene and leads to the loss of FMR1 protein, an mRNA-binding protein and translational inhibitor that is ubiquitously expressed throughout the body with a strong enrichment in neurons (Jin and Warren, 2000; Darnell et al., 2011). Loss of FMR1 function in human and animal models is associated with the excessive growth of dendritic spines (Comery et al., 1997; Irwin et al., 2001; Pan et al., 2004) and defects in synaptic plasticity (Bear et al., 2004; McBride et al., 2005), symptoms also associated with other forms of autism (Hutsler and Zhang, 2010; Tang et al., 2014). Although the defects in animal models of Fragile X syndrome are typically attributed to functions of FMR1 in neurons, the functions of other cell types, such as circulating immune cells in the body or in glia, immune cells in the brain that could also play a role in neurological function, are less well understood.

It is increasingly appreciated that elevated incidences of autism are strikingly correlated with maternal autoimmune diseases and infection during pregnancy (Gesundheit et al., 2013; Estes and McAllister, 2015). As a result, neurological symptoms of autism have been proposed to arise from defects in immune system function, perhaps because of prenatal immune challenges (Mead and Ashwood, 2015). Consistent with this idea, Fragile X syndrome is also associated with altered immune system functions, including elevated proinflammatory cytokine levels in the blood and gastrointestinal inflammation (Samsam et al., 2014; Estes and McAllister, 2015). However, it remains unclear whether defects in immune system functions actively contribute to the progression of Fragile X syndrome or whether they arise independently of the neuronal defects in this disorder. Moreover, the precise defects in other cellular immune functions in Fragile X syndrome models have not been widely investigated.

An essential conserved function of specialized immune cells in *Drosophila melanogaster* and mammals is phagocytosis, or the engulfment of extracellular material generated by foreign pathogens and dying cells (Freeman and Grinstein, 2014). Phagocytosis by immune cells is a multistep process that requires an external signal (e.g., pathogenic bacteria), activation of phagocytic receptors at the cell surface (e.g., CED-1/Draper), rearrangement of the cytoskeleton, and internalization of target material into a subcellular vesicle called the phagosome. Phagosomes undergo subsequent maturation through fusion with endosomes and lysosomes to become acidic phagolysosomes, which degrades the engulfed material. *Drosophila* have several

*R.M. O'Connor and E.F. Stone contributed equally to this paper.

Correspondence to Mimi M. Shirasu-Hiza: ms4095@cumc.columbia.edu

The Rockefeller University Press $30.00
J. Cell Biol. Vol. 216 No. 3 595–605
https://doi.org/10.1083/jcb.201607093

types of phagocytic cells, including primitive macrophages (or hemocytes) in the circulatory system and phagocytic glia in the brain, which play critical roles in defense against bacterial pathogens such as *Streptococcus pneumoniae* and *Serratia marcescens*, the scavenging of dead cellular debris, and the active pruning of neuronal axons and dendrites during development.

Recent research has implicated the misregulation of astrocytes, a type of vertebrate glia, in mouse models of Fragile X syndrome (Jacobs and Doering, 2010; Pacey et al., 2015) and Rett syndrome, another cause of autism spectrum disorder in humans (Ballas et al., 2009; Lioy et al., 2011). For example, astrocytes from *Fmr1* mutant mice cocultured in vitro with neurons from either wild-type or *Fmr1* mutant mice caused excessive dendritic branching, a pathological morphology observed in Fragile X syndrome patients (Jacobs and Doering, 2010). Wild-type astrocytes cocultured in vitro with neurons from wild-type or *Fmr1* mutant mice did not cause this phenotype. Other common neuroanatomical features of Fragile X syndrome patients and animal models include increased dendritic spine density and decreased axonal pruning (Comery et al., 1997; Irwin et al., 2001; Lee et al., 2003; Tessier and Broadie, 2008; Pfeiffer and Huber, 2009). Both of these defects are also associated with defects in glia-mediated phagocytosis (Schafer and Stevens, 2013). Though glia-mediated phagocytosis is required for neuronal structure and function (Blank and Prinz, 2012; Chung and Barres, 2012; Logan et al., 2012), defects in phagocytosis by glia or other immune cells have not previously been demonstrated in any model of Fragile X syndrome.

In this study, we set out to examine immune system function in *Fmr1* mutants, a well-established *Drosophila* model of Fragile X syndrome (Wan et al., 2000; Coffee et al., 2010). We found that *Fmr1* mutants are highly sensitive to infection by two specific bacterial pathogens, *S. pneumoniae* and *S. marcescens*, defense against which requires phagocytosis by hemocytes. We found that hemocytes in *Fmr1* mutants exhibit reduced bacterial engulfment, an early step in phagocytosis. Using tissue-specific RNAi-mediated knockdown, we further show that Fmr1 plays a cell-autonomous role in phagocytosis by hemocytes. In addition, we demonstrate that *Fmr1* mutants exhibited delays in two different processes dependent on phagocytosis by immune cells in the brain: axonal clearance after neuronal wounding in the adult brain and pruning of neurons during development of the mushroom body, a brain structure required for learning and memory. We further found that delayed axonal clearance in the adult was associated with a delay in recruitment of activated, phagocytic glia to the site of wounded neurons. Because glia-mediated phagocytosis is critical in shaping neuronal structure and function (Blank and Prinz, 2012; Chung and Barres, 2012; Logan et al., 2012), these results raise the possibility that delayed phagocytosis by glia may contribute to the neurological symptoms of Fragile X syndrome.

Results and discussion

To investigate immune system function in *Fmr1* mutants, we first analyzed animal survival in response to infection with bacterial pathogens. Defense against bacterial pathogens can be divided into resistance and tolerance mechanisms: resistance mechanisms are conventional immune mechanisms that extend survival by controlling microbial growth, whereas tolerance mechanisms are thought to be physiologies such as metabolic effects that ameliorate the pathogenic effects of infection and do not necessarily alter bacterial loads (Allen et al., 2016). We found that *Fmr1* mutants had resistance phenotypes during infection with *S. pneumoniae* or *S. marcescens* compared with wild types. In both cases, *Fmr1* mutants died more quickly ($P < 0.0001$ for both; Fig. 1, A and B) and had significantly higher bacterial loads relative to wild types 18 h after infection ($P < 0.01$ for both; Fig. 1, C and D). This result suggests that *Fmr1* mutants are less able to control microbial growth of these two bacterial pathogens. *Fmr1* mutants also exhibited wild-type immunity against *Listeria monocytogenes* and sensitivity to *Pseudomonas aeruginosa* infection (Fig. S1, A–D). In contrast to *S. pneumonia* or *S. marcescens* infection, we found no differences in bacterial load after infection with *P. aeruginosa* (Fig. S1, A–D), suggesting that *Fmr1* mutants have a tolerance, not a resistance, phenotype against this infection. These results suggest that Fmr1 affects a resistance mechanism specific to the defense against *S. pneumoniae* and *S. marcescens*, rather than a general immunity defect. To test this, we asked whether *Fmr1* mutants have defects in the Toll and imd pathways, which are well-characterized general mechanisms of immune defense in *Drosophila*. We tested whether the antimicrobial peptides Drosomycin and Diptericin, canonical outputs of the immune signaling Toll and imd pathways, are disrupted in *Fmr1* mutants. Whereas basal expression of these antimicrobial peptides was increased in *Fmr1* mutants, consistent with basal levels of hyperactivated immune function, levels of *Drosomycin* and *Diptericin* expression induced by infection were similar to wild types (Fig. 1, E and F). Thus, *Fmr1* mutants do not display defects in Toll and imd signaling pathways. These results collectively suggest that *Fmr1* mutants are defective in an immune mechanism that specifically compromises the clearance of *S. pneumoniae* and *S. marcescens*.

In *Drosophila*, reduction of bacterial load and survival of infection by *S. pneumoniae* or *S. marcescens* requires phagocytosis by systemic immune cells or hemocytes (Pham et al., 2007; Stone et al., 2012). Phagocytosis involves bacterial engulfment into a vesicle called the phagosome, which fuses with endosomes and eventually with the acidic lysosome. To directly assay the acidic lysosome step of phagocytosis, we performed an in vivo phagocytosis assay by injecting live *Fmr1* mutants and isogenic controls with a well-characterized, commercially available bacterial substrate: heat-inactivated *Staphylococcus aureus* bacteria labeled with a pH-sensitive dye (pHrodo). pHrodo fluorescence increases in acidic environments, and quantification of this signal in phagocytic hemocytes allows quantification of the number of bacteria incorporated into the lysosomal compartment (Stone et al., 2012). We found that *Fmr1* mutants exhibited reduced pHrodo fluorescence in hemocytes compared with wild-type controls, indicating decreased phagocytic activity ($P < 0.01$; Fig. 2 A). To determine whether this decrease in bacterial engulfment results from a decreased phagocytic activity per phagocyte or from a decrease in the number of phagocytes, we genetically labeled hemocytes with GFP using a hemocyte-specific expression driver (Fig. 2, B and C). *Fmr1* mutants again had lower levels of phagocytosis than control flies ($P < 0.01$) but had similar levels of hemocyte GFP expression in the field of view ($P > 0.05$). Thus, when pHrodo fluorescence was normalized to hemocyte GFP expression, *Fmr1* mutants had significantly lower phagocytic activity per hemocyte than did controls ($P < 0.01$). To distinguish whether phagocytosis is disrupted in *Fmr1* mutants at a late step of lysosome acidification or at an

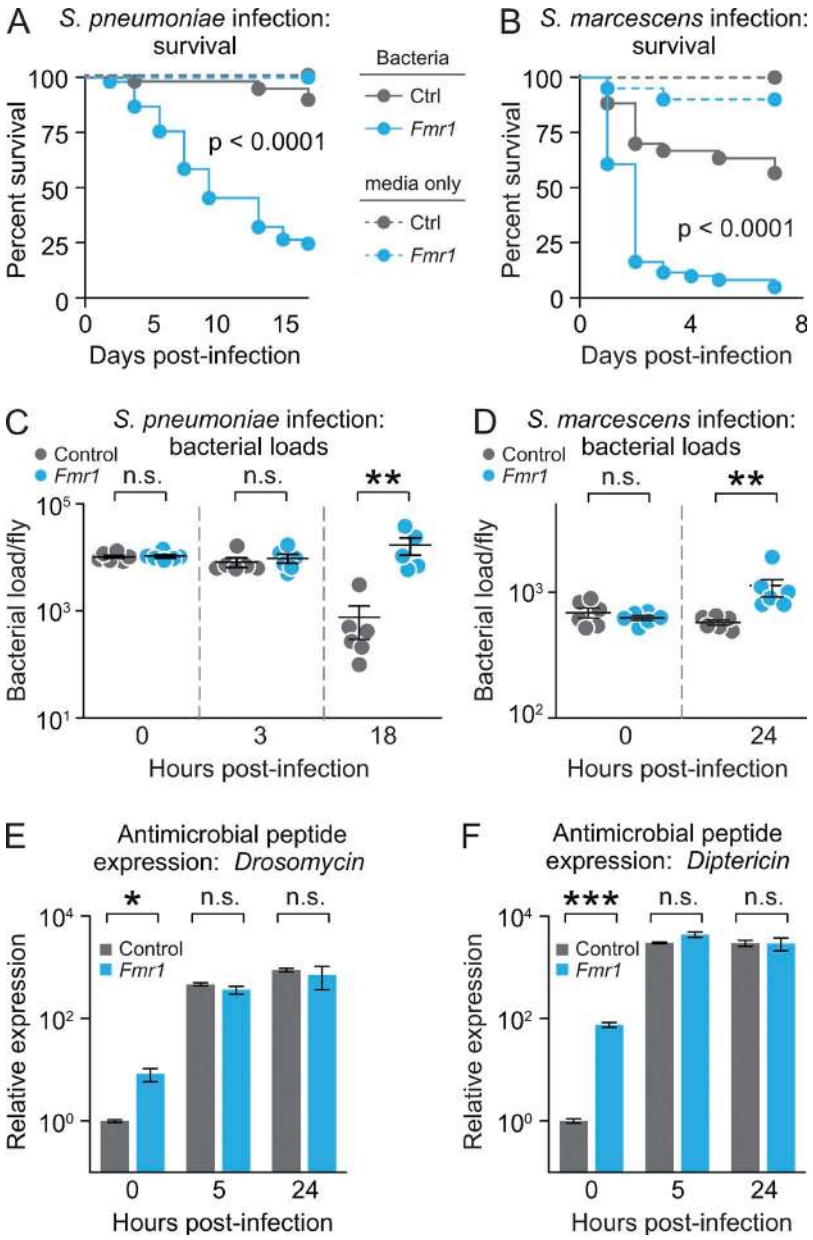

Figure 1. **Immunity against infection is defective in *Fmr1* mutants.** (A and B) Relative to wild-type controls, *Fmr1* mutants are highly sensitive to infection by two bacterial pathogens: *S. pneumoniae* (A; wild type, $n = 59$; *Fmr1*, $n = 53$) and *S. marcescens* (B; wild type, $n = 60$; *Fmr1*, $n = 61$). Ctrl, control. (C and D) Relative to wild-type controls, *Fmr1* mutants are less able to kill and clear these pathogens, as shown by higher bacterial loads at 18 h after infection relative to wild types after infection with *S. pneumoniae* (C; $n = 6$ for each genotype at each time point; $P < 0.01$ at 24 h) and *S. marcescens* (D; $n = 6$ for each genotype at each time point; $P < 0.01$ at 24 h). (E and F) Relative to wild-type controls, *Fmr1* mutants exhibit higher basal expression but similar levels of induced expression of antimicrobial peptides: *Drosomycin*, specific to the Toll pathway (E), and *Diptericin*, specific to the imd pathway (F). Error bars represent SEM. $P = 0.0015$. *, $P < 0.05$; **, $P < 0.01$; ***, $P < 0.001$; not significant (n.s.), $P > 0.05$. (A–F) P-values were obtained by log-rank analysis (A and B), Mann-Whitney *U* test (C and D), or unpaired, two-tailed *t* tests with Welch's correction (E and F). Means ± SEM are shown, and variance is shown by scatter plot.

earlier step, we performed the in vivo phagocytosis assay with Alexa Fluor 594–labeled *S. aureus*. This fluorescence probe tests engulfment, an early step of phagocytosis, and the fluorescence signal from extracellular, nonengulfed bacteria was quenched with Trypan blue, resulting in fluorescence emission only from intracellular, engulfed bacteria. We found that *Fmr1* mutants exhibited decreased intracellular Alexa Fluor 594 fluorescence relative to wild-type controls, indicating that the loss of Fmr1 results in a defect in bacterial engulfment (Figs. 2 D and S2, A and B). To confirm that this defect in phagocytosis is caused by the loss of Fmr1, we compared *Fmr1*-null mutants with *Fmr1*-null mutants containing a transgenic genomic rescue construct of *Fmr1* driven by its endogenous promoter (Fig. S2 C). We found that this transgenic genomic rescue construct was sufficient to increase phagocytic activity. Collectively, these results demonstrate that *Fmr1* is required for the phagocytosis of bacteria by hemocytes.

Fmr1 is expressed ubiquitously throughout the body, and hemocyte function is regulated by many extracellular factors, such as enzymes that process bacteria products and soluble signals from other tissues. To test whether Fmr1 plays a cell-autonomous role in phagocytosis by hemocytes, we performed hemocyte-specific *Fmr1* knockdown by RNAi. We found that flies in which the hemocyte-specific *hemlΔ-Gal4* expression driver was combined with a *UAS-RNAi* construct against *Fmr1* exhibited less phagocytic activity than flies containing either the *hemlΔ-Gal4* driver or the RNAi construct alone (Fig. 3, A and B). Consistent with our results for *Fmr1*-null mutants, when hemocytes were genetically labeled by GFP expression, we found that hemocyte-specific knockdown of Fmr1 did not alter the number of hemocytes (Fig. 3 C). Moreover, similar to *Fmr1*-null mutants, hemocyte-specific knockdown of *Fmr1* caused sensitivity to infection by *S. pneumonie* (Fig. 3 D). Thus, RNAi-mediated knockdown of Fmr1 specifically in hemocytes does not alter the number of hemocytes but causes a defect in their phagocytic activity that results in defective immunity, indicating that Fmr1 plays a cell-autonomous function in phagocytosis by hemocytes.

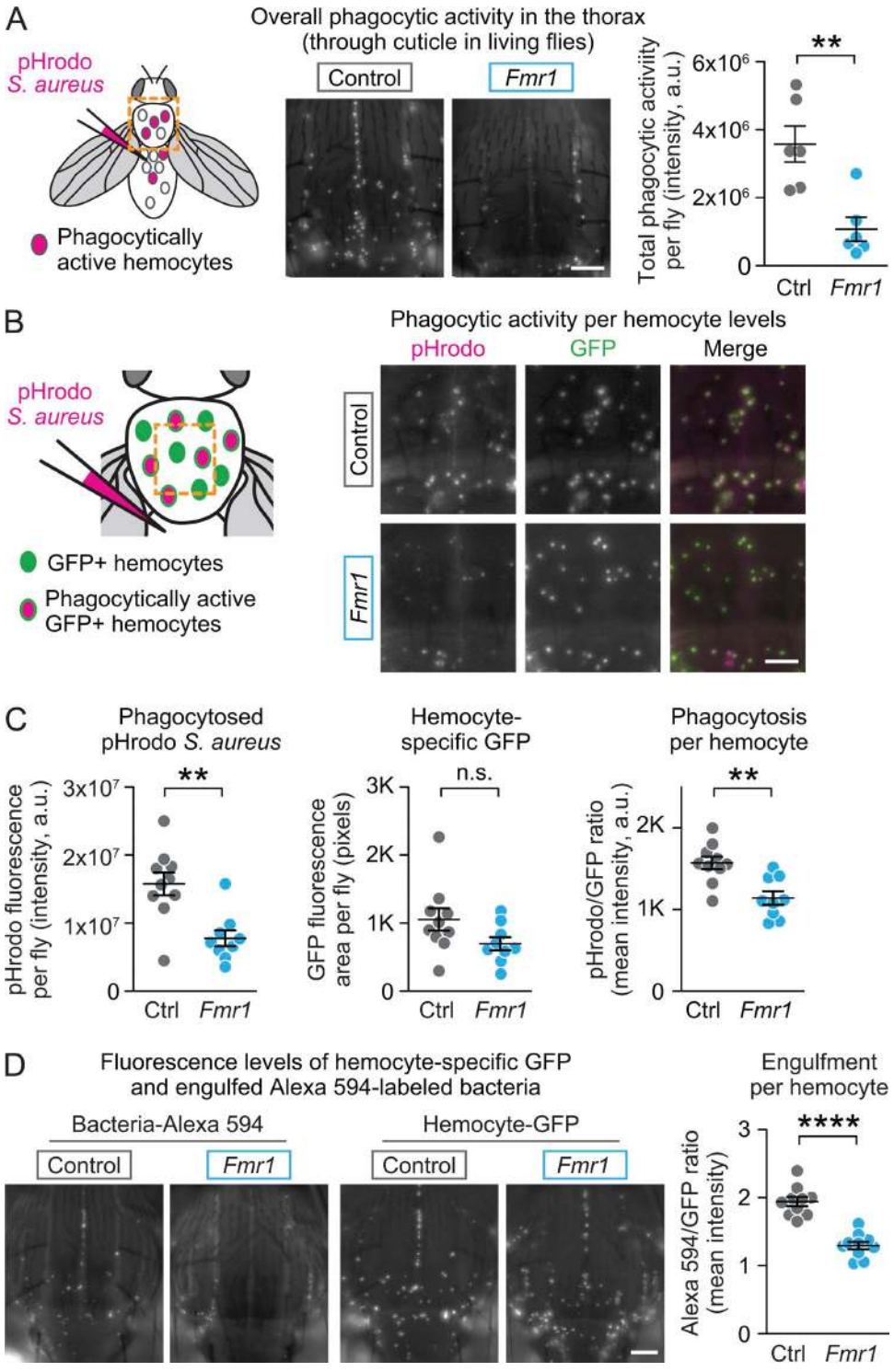

Figure 2. **Phagocytosis by circulating immune cells is defective in *Fmr1* mutants.** (A) *Fmr1* mutants (blue, *n* = 6) exhibit reduced total phagocytosis by immune blood cells (hemocytes) relative to wild types (gray, *n* = 6), as shown by internalization of dead *S. aureus* labeled with pHrodo, a pH-sensitive dye. Shown here are representative fluorescence images and quantifications. (B and C) *Fmr1* mutants exhibit less phagocytic activity per hemocyte. Hemocytes were genetically labeled by *hemlΔ-Gal4* driving *UAS-GFP* expression in both control and *Fmr1* mutants. Shown here are representative fluorescence images (B) and quantification of pHrodo fluorescence (C; wild type, *n* = 10; *Fmr1*, *n* = 9), hemocyte-specific GFP, and phagocytic activity normalized to hemocyte-specific GFP. a.u., arbitrary units. (D) *Fmr1* mutants also exhibit a defect in hemocyte engulfment of *S. aureus*, an early stage of phagocytosis, as measured by the injection of Alexa Fluor 594–labeled dead *S. aureus*, followed by Trypan blue quench (controls, *n* = 10; *Fmr1* mutants, *n* = 10). **, P < 0.01; ****, P < 0.0001; not significant (n.s.), P > 0.05. P-values were obtained by Mann-Whitney *U* test. Means ± SEM are shown, and variance is shown by scatter plot. (A, B, and D) Bars: (A and D) 100 µm; (B) 50 µm.

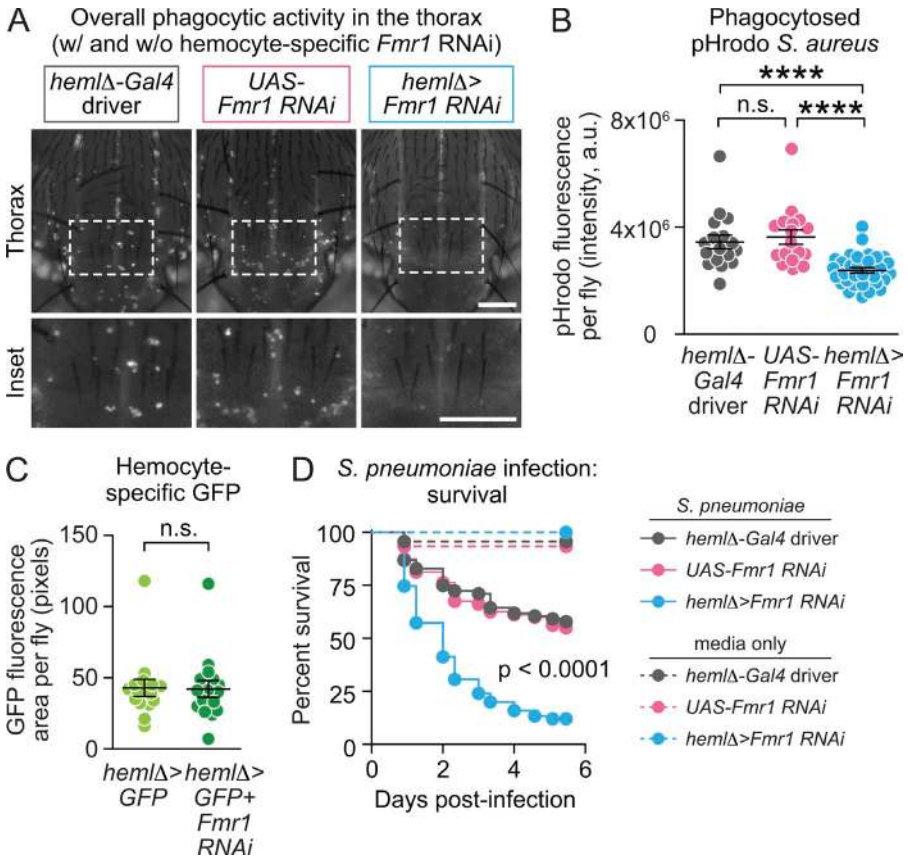

Figure 3. **Fmr1 functions cell autonomously in circulating immune cell phagocytosis.** (A) Shown here are images of overall phagocytic activity in the thoraces of flies containing *hemlΔ-Gal4* driver alone (left), *UAS-Fmr1 RNAi* alone (middle), and *hemlΔ-Gal4* driver expressing *UAS-Fmr1 RNAi* (right). The dashed white rectangles indicate the magnified insets shown below. Bars, 175 mm. (B) Levels of phagocytosed pHrodo *S. aureus* bacteria were quantified per fly for each genotype (n = 17–31 flies per genotype). ****, $P < 0.0001$ for *hemlΔ-Gal4* driver expressing *UAS-Fmr1 RNAi* relative to both controls. a.u., arbitrary units. (C) The hemocyte number in the thorax is not changed by *hemlΔ* driver expression of *Fmr1 RNAi* (n = 15–16 flies per genotype; $P = 0.9335$). (D) Relative to *hemlΔ-Gal4* driver alone (gray) or *Fmr1 RNAi* alone (pink), *hemlΔ-Gal4* driver expressing *Fmr1 RNAi* flies are sensitive to infection by *S. pneumoniae* (*hemlΔ-Gal4* driver alone, n = 80; *Fmr1 RNAi* alone, n = 76; *hemlΔ-driver* expressing *Fmr1 RNAi*, n = 75). (B–D) ****, $P < 0.0001$; not significant (n.s.), $P > 0.05$. P-values were obtained by analysis of variance followed by Tukey's multiple comparison test (B), unpaired t test (C), or log-rank analysis (D). Means ± SEM are shown, and variance is shown by scatter plot.

Because the cellular process of phagocytosis relies on many common molecular components in different cell types, we set out to test whether *Fmr1* mutants also exhibit defects in phagocytosis mediated by immune cells in the brain or glia. We used a neuronal severing (or axotomy) assay to monitor the glia-mediated clearance of neuronal debris in adult animals (Fig. 4; MacDonald et al., 2006). In this assay, the cell-type specific OR85e::GFP marker was used to label a subset of olfactory receptor neurons that extend axons deep into the brain and synapse on olfactory glomeruli (Fig. S3 A). When these axons are severed, the axonal remnants emit an "eat me" signal that activates a subset of phagocytic glia, termed ensheathing glia (Doherty et al., 2009). Activated glia up-regulate expression of the conserved phagocytic receptor Draper and extend membranous processes to the glomeruli to phagocytose neuronal debris (Ziegenfuss et al., 2008, 2012). Clearance of the GFP-labeled neuronal remnants can be quantitatively monitored by loss of GFP signal in the glomeruli (MacDonald et al., 2006). In control animals, the GFP signal from severed neurons was strongly reduced 18 h after axotomy. In contrast, in *Fmr1* mutants, the GFP signal persisted at significantly higher levels 18 h after axotomy ($P < 0.05$; Fig. 4 A). The initial volume of glomeruli was not significantly different between *Fmr1* mutants and controls in unwounded animals ($P > 0.05$; Fig. S3 B). These results indicate that *Fmr1* mutants display defects in the clearance of neuronal remnants after axotomy and suggest that glia-mediated phagocytosis is delayed in these mutants.

Neuronal clearance is dependent on the activation and extension of phagocytic glia to the glomeruli. To determine whether there is a defect in the recruitment of phagocytic glial extensions, we examined the localization of Draper-expressing glia in the region of the glomeruli. Draper, a transmembrane receptor protein of the CED-1 family, is a marker for activated glia that is up-regulated in response to neuronal injury (Ziegenfuss et al., 2012; Doherty et al., 2014). Both *Fmr1* mutants and controls exhibited low levels of Draper protein in the glomeruli of unwounded animals (Fig. S3 C). In control animals, a robust up-regulation of the number of *Draper*-expressing glia in the glomeruli was observed 18 h after axotomy. In contrast, *Fmr1* mutants exhibited significantly lower levels of *Draper*-expressing glia in the glomeruli at this time point ($P < 0.0001$; Fig. 4 B). To extend these results, we then performed experiments to examine the full time course of neuronal clearance (neurons marked by GFP) and *Draper* expression in *Fmr1* mutants and control animals at 0, 12, 18, 24, and 48 h after axotomy. Both neuronal clearance and levels of Draper protein were significantly delayed but not completely inhibited in *Fmr1* mutants (Fig. 4 C). Though activation of Draper expression is thought to be required for the recruitment of activated glial extensions to the site of wounding, it is possible that glial recruitment is normal but that these glia do not express Draper normally in *Fmr1* mutants. To test this, we quantified the ratio of Draper protein per glia by genetically labeling the subset of glia required for clearance of olfactory neurons with RFP. The ratio of Draper to RFP fluorescence was similar between *Fmr1* mutants and control animals after axotomy, indicating that *Draper* expression is not impaired in these glia of *Fmr1* mutants (Figs. 4 D and S3, D and E). That is, the decrease in Draper levels at the glomeruli in *Fmr1* mutants is not caused by decreased *Draper* expression per glia but by decreased numbers of activated phagocytic glia at the glomeruli. Collectively, these results demonstrate that *Fmr1* mutant adults exhibit defects in the recruitment of activated phagocytic glia that lead to delayed neuronal clearance after axotomy.

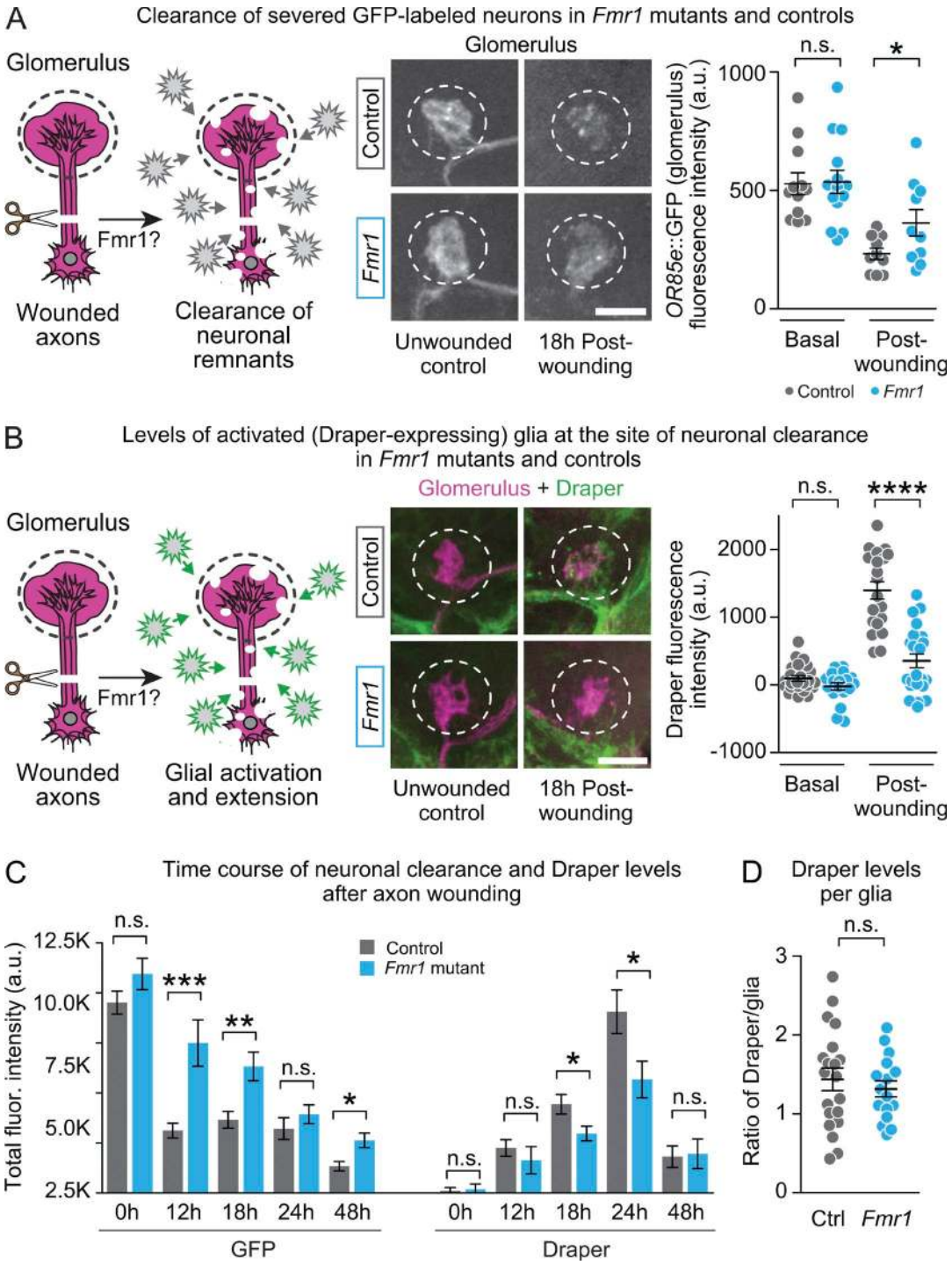

Figure 4. **Glial response to axonal injury is delayed in adult *Fmr1* mutants.** (A) *Fmr1* mutants (n = 10) showed reduced clearance of GFP$^+$ olfactory neurons 18 h after axotomy relative to controls (n = 11). GFP intensity is not different between unwounded controls (control, n = 12; *Fmr1*, n = 14). (B) *Fmr1* mutants (blue, n = 23) showed reduced levels of Draper-expressing glia at the glomeruli 18 h after axotomy relative to controls (gray, n = 20). Draper levels were not different between unwounded controls (control, n = 24; *Fmr1*, n = 18). Bars, 10 µm. (C) *Fmr1* mutants exhibited delays but not total inhibition of axonal clearance and Draper expression in response to neuronal wounding relative to controls. n = 9–14 for each genotype for each time point. (D) The ratio of Draper fluorescence to RFP fluorescence was the same between *Fmr1* mutants and controls, suggesting a defect in activated glial membrane recruitment into the glomeruli rather than a defect in Draper expression. *, $P < 0.05$; **, $P < 0.01$; ***, $P < 0.001$; ****, $P < 0.0001$; not significant (n.s.), $P > 0.05$. P-values were obtained by an unpaired, two-tailed t test with Welch's correction except when the normality test was not passed, in which case the Mann-Whitney U test was used. Means ± SEM are shown, and variance is shown by scatter plot. a.u., arbitrary units; ctrl, control.

Because Fragile X syndrome is a neurodevelopmental disease, we investigated whether *Fmr1* mutants exhibit delays in glia-mediated pruning of neurons during development. One stage of neurodevelopment dependent on glia-mediated phagocytosis is the pruning of γ neurons of the *Drosophila* mushroom body (γ-MB; Fig. S4), a brain structure important for learning

and memory (Tasdemir-Yilmaz and Freeman, 2014). Consistent with previous work, we observed a stereotyped developmental pattern in wild-type animals by immunostaining with anti-FasII antibodies (Fig. 5 A). FasII-positive γ-MB neurons of the dorsal lobe are rapidly pruned in wild-type animals after pupation, with a peak in advanced pruning typically occurring ∼12 h after pupal formation. Advanced pruning is followed by the appearance of FasII-positive α lobe neurons in the same plane (Fushima and Tsujimura, 2007; Awasaki et al., 2011; Tasdemir-Yilmaz and Freeman, 2014). We compared the pruning of FasII-positive γ-MB axons in wild types and *Fmr1* mutants over time (Fig. 5 A). After images were blinded using custom software, the extent of pruning was graded by assignment to one of four morphological classes (examples shown in Fig. 5 A and described in the Developmental glial phagocytosis assay section of Materials and methods). Although *Fmr1* mutants showed similar morphology of FasII-positive γ-MB neurons at 6 h after pupal formation, we found that *Fmr1* mutants exhibited a delay in pruning (Fig. 5 B). At 12 h after pupal formation, ∼75% of wild-type brains exhibited advanced pruning (class III morphology) of FasII-positive γ-MB neurons. In contrast, only ∼30% of *Fmr1* brains exhibited advanced pruning ($P = 0.01$; Fig. 5 C). By 24 h after pupal formation, both wild types and *Fmr1* mutants exhibited similar levels of FasII-positive γ-MB neuronal pruning and FasII-positive α lobe formation. These results suggest that, similar to neuronal clearance after axotomy in adults, development of the mushroom body, a second process that is dependent on glia-mediated phagocytosis, may be delayed in *Fmr1* mutants. Note that overall development is delayed in *Fmr1* mutants, so the delay at this specific stage of mushroom body development may simply reflect a more general delay. Alternatively, delays in glia-mediated phagocytosis may contribute to an overall developmental delay in *Fmr1* mutants.

In summary, our results demonstrate that *Fmr1* mutants exhibit delays in phagocytic immune cells of the brain (glia) and defects in a developmentally independent lineage of blood immune cells in the body (hemocytes). These results provide the first in vivo demonstration of altered immune cell–mediated phagocytosis in a model of Fragile X syndrome. Our results indicate that, in hemocytes, Fmr1 has a cell-autonomous function, but this does not rule out additional nonautonomous roles. *Fmr1* is a broadly expressed translational regulator, with hundreds of known mRNA targets controlling multiple functions, such as cytoskeletal function, cytokine production, and extracellular matrix structure that could regulate phagocytic immune cells. For example, Fmr1 could act cell-autonomously in hemocytes to regulate the expression of specific mRNAs required for the rearrangement of the actin and/or microtubule cytoskeleton; Fmr1 could also play a nonautonomous role in the processing of bacterial products or immune signaling. In glia, Fmr1 could act cell-autonomously as it does in hemocytes, or it could act nonautonomously. Although mRNA targets of Fmr1 specific to glia have not been identified, targets of Fmr1 in whole-brain extracts include small GTPase regulators, microtubule binding proteins, receptor kinase signaling components, and actin itself (Darnell et al., 2011). Fmr1 could also act in neurons to regulate signals that promote phagocytosis by glia or in nonphagocytic glia to modulate the extracellular matrix and to inhibit recruitment of activated glia to severed axons (Suh and Jackson, 2007; Jackson and Haydon, 2008; Patel et al., 2013). Extension of glial processes is known to be dependent on changes in the extracellular matrix such as those stimulated by the secretion of matrix

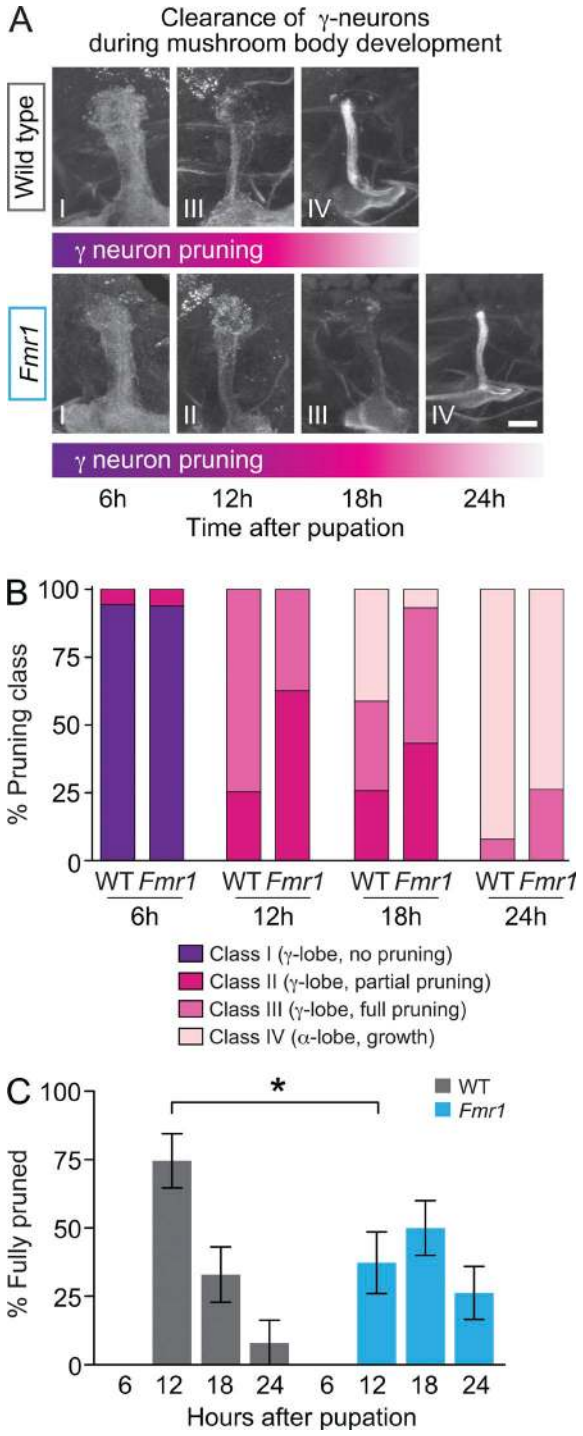

Figure 5. ***Fmr1* mutants exhibit delayed pruning by glia during development.** (A) Images of anti-FasII staining of the developing mushroom body in wild-type (gray) and *Fmr1* (blue) mutants at 6, 12, 18, and 24 h after pupation show the delayed pruning of FasII-positive γ-MB neurons in the dorsal lobe in *Fmr1* mutants relative to wild types. Roman numerals refer to phenotypic pruning classes shown in B. Bar, 10 µm. (B) The distribution of morphological phenotypes over time shows an increased percentage of *Fmr1* mutants with partial pruning phenotypes at 12 and 18 h after pupation relative to wild types (WT; averages of three trials, total $n = 25–50$ per genotype per time point). (C) At 12 h after pupation, wild-type flies exhibit a significantly higher percentage of structures (75%) with advanced pruning morphology than *Fmr1* mutants (37%; $n = 3$ trials; total wild type, $n = 50$; total *Fmr1* mutants, $n = 33$). *, $P < 0.05$. The p-value was obtained by an unpaired, two-tailed *t* test with Welch's correction. The mean ± SD is shown.

metalloproteinases which have been implicated in Fragile X syndrome (Siller and Broadie, 2012). Fmr1 might also act either at the time of phagocytic activation or much earlier during development. Both the timing and tissue-specific location of Fmr1 activities required for phagocytosis by immune cells, particularly glia, remain important questions for future investigation.

It remains to be investigated whether phagocytic defects could also contribute to the neurological and immunological symptoms associated with Fragile X syndrome in human patients and whether phagocytic defects exist in other types of autism spectrum disorder. Although early detection of autism spectrum disorder has been shown to be critical for effective therapeutic intervention, autism spectrum disorders that are not attributed to monogenic causes such as Fragile X syndrome or Rett syndrome can be extremely difficult to diagnose at a young age. If the neuroanatomical pruning defects common to many types of autism spectrum disorder are caused in part by defects that manifest both in phagocytic immune cells of the brain and blood, these shared features could provide a strategy to screen for phagocytic biomarkers or bioactivities in easily obtainable blood immune cells from young patients at risk.

Materials and methods

Fly lines

Fmr1 trans-heterozygous null mutants were generated by crossing two heterozygous mutant lines, and each contained a well-characterized *Fmr1*-null mutation. $Fmr1^{\Delta 50M}$ was from D. Zarnescu (Zarnescu et al., 2005), and $Fmr1^{3}$ was from T. Jongens (Wan et al., 2000). Both *Fmr1* mutant lines were outcrossed to their wild-type controls (Oregon R and iso31b, respectively) for at least six generations. For all experiments with *Fmr1*-null mutants, wild-type controls were generated by crossing Oregon R and iso31b lines and collecting the heterozygous progeny. Hemocytes were labeled with GFP using a *hemlΔ-Gal4* construct paired with *UAS-GFP*. For hemocyte-specific RNAi of dFMR1, the *hemlΔ-Gal4* driver was used to drive expression of *UAS-Fmr1-RNAi* (identification no. 8933; Vienna Drosophila Resource Center). The *hemlΔ-Gal4* and *UAS-Fmr1-RNAi* constructs were outcrossed to W^{1118} Canton-S for 10 and 6 generations, respectively, and W^{1118} Canton-S flies were used as controls. Olfactory neurons were labeled using the *OR85e::mCD8-GFP* construct from M. Freeman (Doherty et al., 2009). Ensheathing glia were labeled with an *mz0709-Gal4* construct from M. Freeman (Doherty et al., 2009) paired with *UAS-RFP*. These transgenic constructs were also outcrossed for six to eight generations with appropriate wild-type control strains to maintain proper genetic backgrounds for experimental use.

Bacterial strains

Bacterial infections were performed with four types of bacteria: *S. pneumoniae* strain SP1, a streptomycin-resistant variant of D39, from S. Falkow (Joyce et al., 2004); *S. marcescens* strain DB1140 from M.W. Tan (Genentech, San Francisco, CA; Flyg and Xanthopoulos, 1983); *L. monocytogenes* strain 10403S from J. Theriot (Stanford University, Stanford, CA; Mansfield et al., 2003); and *P. aeruginosa* from B. Lazzaro (Cornell University, Ithaca, NY).

Fly rearing conditions

Flies were raised at 25°C and 55% humidity on yeasted, low-glutamate food in a 12:12 h light/dark cycle (Chang et al., 2008). Flies collected for survival and hemocyte phagocytosis experiments were maintained on standard dextrose food. The recipe for standard dextrose food is as follows: 38 g/liter cornmeal, 20.5 g/liter yeast, 85.6 g/liter dextrose, and 7.1 g/liter agar. Infection experiments were performed with age-matched male flies 5–7 d after eclosion. Glial phagocytosis experiments were performed with age-matched females 5–10 d after eclosion that were maintained on low-glutamate food before and after maxillary palp excision.

Statistical analysis

Statistical analyses were performed using Prism (GraphPad Software). When comparing two groups of quantitative data, an unpaired, two-tailed *t* test with Welch's correction was performed if data showed a normal distribution (determined using the D'Agostino and Pearson omnibus normality test) and the Mann-Whitney *U* test if data distribution was nonnormal. Survival data were analyzed using log-rank analysis.

Infections

Infection experiments were performed as previously described (Stone et al., 2012). In brief, flies were grown at 25°C, anesthetized on CO_2 pads, and injected using a custom microinjector (MINJ-Fly; Tritech) and glass capillary needles pulled with a vertical micropipette puller (P-30; Sutter Instrument). 50 nl of liquid were injected into each fly, calibrated by measuring the diameter of the expelled drop under oil. *S. pneumoniae* cultures were grown to an OD_{600} of 0.40 at 37°C + 5% CO_2 in standing tryptic soy media and frozen in 5% glycerol at −80°C. For infection, bacteria were pelleted and upon thawing, supernatant was removed, and the pellet was resuspended in fresh brain–heart infusion (BHI) media and diluted to a final OD_{600} of 0.10–0.12 for injection. *S. marcescens* was grown in shaking BHI overnight at 37°C and diluted to OD_{600} ranging from 0.1 to 0.6 for injection into flies. *L. monocytogenes* was grown in standing BHI overnight at 37°C and diluted to a final OD_{600} of 0.1 for injection. *P. aeruginosa* was grown in shaking lysogeny broth overnight at 37°C and diluted to a final OD_{600} of 1.0 for injection. After injection, flies were incubated at 29°C in a 12:12 h light/dark cycle for the duration of the infection.

Survival assays

Between 60 and 85 flies per genotype per condition were assayed for each survival curve and placed in three vials of standard dextrose food with ∼20 flies each. In each experiment, 20–40 flies of each line were also injected with sterile media as a control for death by wounding. Survival proportions were assayed by counting the number of dead flies at various time points after infection. Data were converted to Kaplan-Meier format using a custom Excel-based software called Count the Dead from J. Shirasu-Hiza (Microsoft; Stone et al., 2012). Survival curves were plotted as Kaplan-Meier plots, and statistical significance was tested using log-rank analysis with Prism software. All experiments were performed at least three times and yielded similar results.

Bacterial load quantitation

Six individual flies were collected at each time point after microbial challenge. These flies were homogenized in sterile PBS, diluted serially, and plated on tryptic soy blood agar plates (*S. pneumoniae*) or lysogeny broth agar plates (*S. marcescens*). Statistical significance was determined using unpaired, two-tailed *t* tests for 0-h time points and nonparametric Mann-Whitney *U* tests for all other time points to account for exponential growth. All experiments were performed at least three times and yielded similar results.

Assay of phagocytosis by immune blood cells

Male flies 5–7 d old were injected with 50 nl of 20 mg/ml pHrodo-labeled *S. aureus* in PBS (A10010) or Alexa Fluor 594–labeled *S. aureus* in PBS (S23372; Molecular Probes). The flies were allowed to

phagocytose the particles for 35–45 min. Using a thin layer of Loctite superglue, the dorsal surfaces of the flies were glued onto coverslips; for experiments using Alexa Fluor 594–labeled bacteria, nonphagocytosed bacteria were quenched by Trypan blue injection (~100 nl) into the circulating hemolymph. Fluorescence images were taken of the dorsal surface using epifluorescence illumination with a microscope (Eclipse E800; Nikon) fitted with a Cool Snaps HQ^2 camera (Photometrics) with 10× or 20× objectives. Images were captured and quantified using Elements software (Nikon). To quantify, all of the images within an experiment were thresholded using the same pixel intensity value to define regions of interest; the sum and mean intensities of the regions of interest were then calculated. Experiments were repeated three times with 6–14 flies for each treatment. For determination of the number of pHrodo-labeled positive hemocytes, the local maxima tool was used for particle counting in FIJI software suite (ImageJ; National Institutes of Health). Assays examining total phagocyte numbers were performed using flies expressing a UAS-GFP construct with the hemocyte-specific promoter *hemlΔ-Gal4*. Statistical significance was determined using unpaired, two-tailed *t* tests.

Glial phagocytosis assay and immunohistochemistry

Glial phagocytosis assays were conducted as described previously (MacDonald et al., 2006) with some modifications. The maxillary palps of age-matched 5–10-d-old OR85e::mCD8-GFP (from M. Freeman); *Fmr1$^{3/\Delta 50M}$* mutants and wild-type controls were excised to sever the olfactory neurons. Flies were collected and decapitated at various time points after wounding, and the fly heads were fixed for 40 min at room temperature in 4% PFA in PBS + 0.1% Triton X-100 (PTX). Fly heads were washed five times in PTX, and brains were dissected in ice-cold PTX. Brains were blocked in 4% normal donkey serum (NDS) in PTX for 1 h and incubated in primary antibodies at 4°C overnight. Primary antibodies were diluted in PTX with 2% NDS. The following primary antibodies and dilutions were used: rabbit anti-Draper (1:500; from M. Freeman; MacDonald et al., 2006), chicken anti-GFP (1:1,000; 13970; Abcam), and mouse anti-RFP (1:500; 65856; Abcam). Brains were then washed five times over the course of 1 h at room temperature in PTX and incubated in secondary antibodies at 4°C overnight. Secondary antibodies were diluted in PTX with 2% NDS. The following secondary antibodies and dilutions were used: Rhodamine red-X–conjugated donkey anti–rabbit IgG (1:200; 711-295-152), Alexa Fluor 488–conjugated donkey anti–chicken IgY (IgG; 1:200; 703-545-155), Rhodamine red-X–conjugated donkey anti–mouse IgG (1:200; 715-295-151), and Alexa Fluor 647–conjugated donkey anti–rabbit (1:200; 711-605-152; Jackson ImmunoResearch Laboratories, Inc.). Brains were washed and mounted onto coverslips that had been coated with poly-L-lysine (5048; Advanced BioMatrix) and Photo Flo 200 (0.36%; 1464510; Kodak), were dehydrated by incubation in increasing concentrations of ethanol for 5 min (30, 50, 75, 95, and 100%), and then were incubated in two different solutions of 100% xylenes for 10 min each. Coverslips were mounted onto slides with distyrene plasticizer xylene (DPX) and dried overnight before imaging. Brains were imaged using an LSM 510 Meta upright confocal microscope (ZEISS) using 488-, 561-, and 633-nm lasers. Images were taken with a PlanNeoFL 40×/1.3 NA lens, and the LSM confocal software was used for 3D reconstruction. FIJI was used to quantify the total fluorescence intensity of the three middle slices in a region traced around each glomerulus, normalizing to background fluorescence for each sample. For the glial extension assay, fluorescence of ensheathing glia and Draper was quantified using a standard circular region of interest placed over the glomerulus, normalizing to background fluorescence for each sample. All experiments were performed at least three times and yielded similar results. Statistical significance was determined using unpaired, two-tailed *t* tests.

Developmental glial phagocytosis assay

Fmr1$^{3/\Delta 50M}$ mutants and wild-type controls were raised as described in the Fly lines and Fly rearing conditions sections and were collected at various time points after pupal formation. The pupae were fixed in two 15-min washes in 4% PFA in PTX. They were then washed, stained, and imaged as described in the Glial phagocytosis and immunohistochemistry section. Antibodies used were mouse anti-FasII (1:5; DSHB 1D4) and Alexa Fluor 488–conjugated donkey anti–mouse IgG (1:200; 715–545-151; Jackson ImmunoResearch Laboratories, Inc.). Maximum intensity projections were generated, and images were blinded with a randomized numbering system using a custom-built blinding script developed by T. Khan (Columbia University, New York, NY) and then scored based on the following criteria: no pruning (class I), partial pruning (class II), advanced pruning (class III), and α lobe growth (class IV). Examples for each class are shown in Fig. 5 A as the wild-type images for the 6 h (class I), 12 h (class III), and 18 h (class IV) after pupation, as well as the *Fmr1* image for 12 h (class II). Samples were unblinded and results recorded. The percentages in each category were calculated for each genotype at each time point; mean percentages were then calculated with three independent trials. Statistical significance was determined using unpaired, two-tailed *t* tests.

Online supplemental material

Fig. S1 shows that Fmr1 mutants exhibit wild-type bacterial loads after infection with *P. aeruginosa* and *L. monocytogenes*. Fig. S2 shows that Fmr1 mutants have a defect in phagocytic engulfment that can be rescued by Fmr1 expression. Fig. S3 shows that the glomeruli of Fmr1 mutants and controls are similar in the unwounded state and that Fmr1 mutants exhibit less recruitment of activated glia after wounding. Fig. S4 shows anti-Corazonin staining of the dissected ventral nerve cord and mushroom bodies in the developing brain.

Acknowledgments

We thank all Shirasu-Hiza, Grueber, and Canman laboratory members for support. We also thank Thomas Khan for custom sample-blinding software; Adam Ryan, Albert Kim, and Paul Kim for technical support; and Gerard Karsenty and Rodney Rothstein for equipment use.

This work was supported by National Institutes of Health grants F31NS080673 (to E.F. Stone); R01GM117407 and DP2OD008773 (to J.C. Canman); and R01GM105775 and R01AG045842 (to M.M. Shirasu-Hiza); and a Hirschl Foundation grant to M.M. Shirasu-Hiza.

The authors declare no competing financial interests.

Author contributions: M.M Shirasu-Hiza, R.M. O'Connor, E.F. Stone, C.R. Wayne, and E.V. Marcinkevicius designed experiments. Experiments were performed and analyzed by R.M. O'Connor (Figs. 1, 4, 5, and S4); E.F. Stone (Figs. 1, 2, 4, and S1); C.R. Wayne (Figs. 5 and S3); E.V. Marcinkevicius (Figs. 2 and S2); M. Ulgherait, R. Delventhal, M.M. Pantalia, V.M. Hill, S. McAllister, and A. Chen (Figs. 3 and S2); and C.G. Zhou (Figs. 1 and S1). J.S. Ziegenfuss, W.B. Grueber, and J.C. Canman provided technical support and intellectual contributions. M.M. Shirasu-Hiza, J.C. Canman, R.M. O'Connor, and C.R. Wayne wrote the manuscript with feedback from E.F. Stone, J.S. Ziegenfuss, E.V. Marcinkevicius, and W.B. Grueber.

Submitted: 23 July 2016
Revised: 22 November 2016
Accepted: 30 January 2017

References

Allen, V.W., R.M. O'Connor, M. Ulgherait, C.G. Zhou, E.F. Stone, V.M. Hill, K.R. Murphy, J.C. Canman, W.W. Ja, and M.M. Shirasu-Hiza. 2016. *period*-regulated feeding behavior and TOR signaling modulate survival of infection. *Curr. Biol.* 26:184–194 (published erratum appears in *Curr. Biol.* 2016. 26:1383). http://dx.doi.org/10.1016/j.cub.2015.11.051

Awasaki, T., Y. Huang, M.B. O'Connor, and T. Lee. 2011. Glia instruct developmental neuronal remodeling through TGF-β signaling. *Nat. Neurosci.* 14:821–823. http://dx.doi.org/10.1038/nn.2833

Ballas, N., D.T. Lioy, C. Grunseich, and G. Mandel. 2009. Non-cell autonomous influence of MeCP2-deficient glia on neuronal dendritic morphology. *Nat. Neurosci.* 12:311–317. http://dx.doi.org/10.1038/nn.2275

Bear, M.F., K.M. Huber, and S.T. Warren. 2004. The mGluR theory of fragile X mental retardation. *Trends Neurosci.* 27:370–377. http://dx.doi.org/10.1016/j.tins.2004.04.009

Blank, T., and M. Prinz. 2012. Microglia as modulators of cognition and neuropsychiatric disorders. *Glia.*61:62–70 https://doi.org/10.1002/glia.22372

Chang, S., S.M. Bray, Z. Li, D.C. Zarnescu, C. He, P. Jin, and S.T. Warren. 2008. Identification of small molecules rescuing fragile X syndrome phenotypes in *Drosophila*. *Nat. Chem. Biol.* 4:256–263. http://dx.doi.org/10.1038/nchembio.78

Chung, W.S., and B.A. Barres. 2012. The role of glial cells in synapse elimination. *Curr. Opin. Neurobiol.* 22:438–445. http://dx.doi.org/10.1016/j.conb.2011.10.003

Coffee, R.L. Jr., C.R. Tessier, E.A. Woodruff III, and K. Broadie. 2010. Fragile X mental retardation protein has a unique, evolutionarily conserved neuronal function not shared with FXR1P or FXR2P. *Dis. Model. Mech.* 3:471–485. http://dx.doi.org/10.1242/dmm.004598

Comery, T.A., J.B. Harris, P.J. Willems, B.A. Oostra, S.A. Irwin, I.J. Weiler, and W.T. Greenough. 1997. Abnormal dendritic spines in fragile X knockout mice: maturation and pruning deficits. *Proc. Natl. Acad. Sci. USA.* 94:5401–5404. http://dx.doi.org/10.1073/pnas.94.10.5401

Darnell, J.C., S.J. Van Driesche, C. Zhang, K.Y. Hung, A. Mele, C.E. Fraser, E.F. Stone, C. Chen, J.J. Fak, S.W. Chi, et al. 2011. FMRP stalls ribosomal translocation on mRNAs linked to synaptic function and autism. *Cell.* 146:247–261. http://dx.doi.org/10.1016/j.cell.2011.06.013

Doherty, J., M.A. Logan, O.E. Taşdemir, and M.R. Freeman. 2009. Ensheathing glia function as phagocytes in the adult *Drosophila* brain. *J. Neurosci.* 29:4768–4781. http://dx.doi.org/10.1523/JNEUROSCI.5951-08.2009

Doherty, J., A.E. Sheehan, R. Bradshaw, A.N. Fox, T.Y. Lu, and M.R. Freeman. 2014. PI3K signaling and Stat92E converge to modulate glial responsiveness to axonal injury. *PLoS Biol.* 12. http://dx.doi.org/10.1371/journal.pbio.1001985

Estes, M.L., and A.K. McAllister. 2015. Immune mediators in the brain and peripheral tissues in autism spectrum disorder. *Nat. Rev. Neurosci.* 16:469–486. http://dx.doi.org/10.1038/nrn3978

Flyg, C., and K. Xanthopoulos. 1983. Insect pathogenic properties of *Serratia marcescens*. Passive and active resistance to insect immunity studied with protease-deficient and phage-resistant mutants. *J. Gen. Microbiol.* 129:453–464.

Freeman, S.A., and S. Grinstein. 2014. Phagocytosis: receptors, signal integration, and the cytoskeleton. *Immunol. Rev.* 262:193–215. http://dx.doi.org/10.1111/imr.12212

Fushima, K., and H. Tsujimura. 2007. Precise control of *fasciclin II* expression is required for adult mushroom body development in *Drosophila*. *Dev. Growth Differ.* 49:215–227. http://dx.doi.org/10.1111/j.1440-169X.2007.00922.x

Gesundheit, B., J.P. Rosenzweig, D. Naor, B. Lerer, D.A. Zachor, V. Procházka, M. Melamed, D.A. Kristt, A. Steinberg, C. Shulman, et al. 2013. Immunological and autoimmune considerations of autism spectrum disorders. *J. Autoimmun.* 44:1–7. http://dx.doi.org/10.1016/j.jaut.2013.05.005

Hutsler, J.J., and H. Zhang. 2010. Increased dendritic spine densities on cortical projection neurons in autism spectrum disorders. *Brain Res.* 1309:83–94. http://dx.doi.org/10.1016/j.brainres.2009.09.120

Irwin, S.A., B. Patel, M. Idupulapati, J.B. Harris, R.A. Crisostomo, B.P. Larsen, F. Kooy, P.J. Willems, P. Cras, P.B. Kozlowski, et al. 2001. Abnormal dendritic spine characteristics in the temporal and visual cortices of patients with fragile-X syndrome: a quantitative examination. *Am. J. Med. Genet.* 98:161–167. http://dx.doi.org/10.1002/1096-8628(20010115)98:2<161::AID-AJMG1025>3.0.CO;2-B

Jackson, F.R., and P.G. Haydon. 2008. Glial cell regulation of neurotransmission and behavior in *Drosophila*. *Neuron Glia Biol.* 4:11–17. http://dx.doi.org/10.1017/S1740925X09000027

Jacobs, S., and L.C. Doering. 2010. Astrocytes prevent abnormal neuronal development in the fragile X mouse. *J. Neurosci.* 30:4508–4514. http://dx.doi.org/10.1523/JNEUROSCI.5027-09.2010

Jin, P., and S.T. Warren. 2000. Understanding the molecular basis of fragile X syndrome. *Hum. Mol. Genet.* 9:901–908. http://dx.doi.org/10.1093/hmg/9.6.901

Joyce, E.A., A. Kawale, S. Censini, C.C. Kim, A. Covacci, and S. Falkow. 2004. LuxS is required for persistent pneumococcal carriage and expression of virulence and biosynthesis genes. *Infect. Immun.* 72:2964–2975. http://dx.doi.org/10.1128/IAI.72.5.2964-2975.2004

Kelleher, R.J. III, and M.F. Bear. 2008. The autistic neuron: troubled translation? *Cell.* 135:401–406. http://dx.doi.org/10.1016/j.cell.2008.10.017

Lee, A., W. Li, K. Xu, B.A. Bogert, K. Su, and F.B. Gao. 2003. Control of dendritic development by the *Drosophila fragile X*-related gene involves the small GTPase Rac1. *Development.* 130:5543–5552. http://dx.doi.org/10.1242/dev.00792

Lioy, D.T., S.K. Garg, C.E. Monaghan, J. Raber, K.D. Foust, B.K. Kaspar, P.G. Hirrlinger, F. Kirchhoff, J.M. Bissonnette, N. Ballas, and G. Mandel. 2011. A role for glia in the progression of Rett's syndrome. *Nature.* 475:497–500. http://dx.doi.org/10.1038/nature10214

Logan, M.A., R. Hackett, J. Doherty, A. Sheehan, S.D. Speese, and M.R. Freeman. 2012. Negative regulation of glial engulfment activity by Draper terminates glial responses to axon injury. *Nat. Neurosci.* 15:722–730. http://dx.doi.org/10.1038/nn.3066

MacDonald, J.M., M.G. Beach, E. Porpiglia, A.E. Sheehan, R.J. Watts, and M.R. Freeman. 2006. The *Drosophila* cell corpse engulfment receptor Draper mediates glial clearance of severed axons. *Neuron.* 50:869–881. http://dx.doi.org/10.1016/j.neuron.2006.04.028

Mansfield, B.E., M.S. Dionne, D.S. Schneider, and N.E. Freitag. 2003. Exploration of host-pathogen interactions using *Listeria monocytogenes* and *Drosophila melanogaster*. *Cell. Microbiol.* 5:901–911. http://dx.doi.org/10.1046/j.1462-5822.2003.00329.x

McBride, S.M., C.H. Choi, Y. Wang, D. Liebelt, E. Braunstein, D. Ferreiro, A. Sehgal, K.K. Siwicki, T.C. Dockendorff, H.T. Nguyen, et al. 2005. Pharmacological rescue of synaptic plasticity, courtship behavior, and mushroom body defects in a *Drosophila* model of fragile X syndrome. *Neuron.* 45:753–764. http://dx.doi.org/10.1016/j.neuron.2005.01.038

Mead, J., and P. Ashwood. 2015. Evidence supporting an altered immune response in ASD. *Immunol. Lett.* 163:49–55. http://dx.doi.org/10.1016/j.imlet.2014.11.006

Pacey, L.K., S. Guan, S. Tharmalingam, C. Thomsen, and D.R. Hampson. 2015. Persistent astrocyte activation in the fragile X mouse cerebellum. *Brain Behav.* 5. http://dx.doi.org/10.1002/brb3.400

Pan, L., Y.Q. Zhang, E. Woodruff, and K. Broadie. 2004. The *Drosophila* fragile X gene negatively regulates neuronal elaboration and synaptic differentiation. *Curr. Biol.* 14:1863–1870. http://dx.doi.org/10.1016/j.cub.2004.09.085

Patel, A.B., S.A. Hays, I. Bureau, K.M. Huber, and J.R. Gibson. 2013. A target cell-specific role for presynaptic *Fmr1* in regulating glutamate release onto neocortical fast-spiking inhibitory neurons. *J. Neurosci.* 33:2593–2604. http://dx.doi.org/10.1523/JNEUROSCI.2447-12.2013

Pfeiffer, B.E., and K.M. Huber. 2009. The state of synapses in fragile X syndrome. *Neuroscientist.* 15:549–567. http://dx.doi.org/10.1177/1073858409333075

Pham, L.N., M.S. Dionne, M. Shirasu-Hiza, and D.S. Schneider. 2007. A specific primed immune response in *Drosophila* is dependent on phagocytes. *PLoS Pathog.* 3. http://dx.doi.org/10.1371/journal.ppat.0030026

Samsam, M., R. Ahangari, and S.A. Naser. 2014. Pathophysiology of autism spectrum disorders: revisiting gastrointestinal involvement and immune imbalance. *World J. Gastroenterol.* 20:9942–9951. http://dx.doi.org/10.3748/wjg.v20.i29.9942

Schafer, D.P., and B. Stevens. 2013. Phagocytic glial cells: sculpting synaptic circuits in the developing nervous system. *Curr. Opin. Neurobiol.* 23:1034–1040. http://dx.doi.org/10.1016/j.conb.2013.09.012

Siller, S.S., and K. Broadie. 2012. Matrix metalloproteinases and minocycline: therapeutic avenues for fragile X syndrome. *Neural Plast.* 2012.

Stone, E.F., B.O. Fulton, J.S. Ayres, L.N. Pham, J. Ziauddin, and M.M. Shirasu-Hiza. 2012. The circadian clock protein timeless regulates phagocytosis of bacteria in *Drosophila*. *PLoS Pathog.* 8. http://dx.doi.org/10.1371/journal.ppat.1002445

Suh, J., and F.R. Jackson. 2007. *Drosophila* ebony activity is required in glia for the circadian regulation of locomotor activity. *Neuron.* 55:435–447. http://dx.doi.org/10.1016/j.neuron.2007.06.038

Tang, G., K. Gudsnuk, S.H. Kuo, M.L. Cotrina, G. Rosoklija, A. Sosunov, M.S. Sonders, E. Kanter, C. Castagna, A. Yamamoto, et al. 2014. Loss of mTOR-dependent macroautophagy causes autistic-like synaptic pruning deficits. *Neuron.* 83:1131–1143 (published erratum appears in *Neuron*. 2014. 83:1482). http://dx.doi.org/10.1016/j.neuron.2014.07.040

Tasdemir-Yilmaz, O.E., and M.R. Freeman. 2014. Astrocytes engage unique molecular programs to engulf pruned neuronal debris from distinct subsets of neurons. *Genes Dev.* 28:20–33. http://dx.doi.org/10.1101/gad.229518.113

Tessier, C.R., and K. Broadie. 2008. *Drosophila* fragile X mental retardation protein developmentally regulates activity-dependent axon pruning. *Development.* 135:1547–1557. http://dx.doi.org/10.1242/dev.015867

Wan, L., T.C. Dockendorff, T.A. Jongens, and G. Dreyfuss. 2000. Characterization of dFMR1, a *Drosophila melanogaster* homolog of the fragile X mental retardation protein. *Mol. Cell. Biol.* 20:8536–8547. http://dx.doi.org/10.1128/MCB.20.22.8536-8547.2000

Zarnescu, D.C., P. Jin, J. Betschinger, M. Nakamoto, Y. Wang, T.C. Dockendorff, Y. Feng, T.A. Jongens, J.C. Sisson, J.A. Knoblich, et al. 2005. Fragile X protein functions with Lgl and the PAR complex in flies and mice. *Dev. Cell.* 8:43–52. http://dx.doi.org/10.1016/j.devcel.2004.10.020

Ziegenfuss, J.S., R. Biswas, M.A. Avery, K. Hong, A.E. Sheehan, Y.G. Yeung, E.R. Stanley, and M.R. Freeman. 2008. Draper-dependent glial phagocytic activity is mediated by Src and Syk family kinase signalling. *Nature.* 453:935–939. http://dx.doi.org/10.1038/nature06901

Ziegenfuss, J.S., J. Doherty, and M.R. Freeman. 2012. Distinct molecular pathways mediate glial activation and engulfment of axonal debris after axotomy. *Nat. Neurosci.* 15:979–987. http://dx.doi.org/10.1038/nn.3135